IEEE Access
Multidisciplinary ⋮ Rapid Review ⋮ Open Access Journal

Received November 22, 2020, accepted December 1, 2020, date of publication December 9, 2020,
date of current version December 24, 2020.

Digital Object Identifier 10.1109/ACCESS.2020.3043413

Combining Statistical Features and Local Pattern Features for Texture Image Retrieval

HENGBIN WANG, HUAIJING QU, JIA XU, JIWEI WANG, YANAN WEI, AND ZHISHENG ZHANG
School of Information & Electric Engineering, Shandong Jianzhu University, Jinan 250101, China
Corresponding author: Huaijing Qu (quhuaijing@sdjzu.edu.cn)

This work was supported by the Shandong Provincial Natural Science Foundation of China under Grant ZR2014FM016.

ABSTRACT The complementary fusion of global and local features can effectively improve the performance of image retrieval. This article proposes a new local texture descriptor, combined with statistical modeling in transform domain for texture image retrieval. The proposed local descriptor calculates the eight directions of the central pixel by using the relationship between the central pixel and the neighboring pixels in six directions, which is called the local eight direction pattern (LEDP). In the texture image retrieval system of this article, the feature extraction part combines global statistical features and local pattern features. Among them, both the relative magnitude (RM) sub-band coefficients and relative phase (RP) sub-band coefficients are modeled as wrapped Cauchy (WC) distribution in the dual-tree complex wavelet transform (DTCWT) domain, and the global statistical features employ the parameters of this model; while the local pattern features respectively choose the local binary pattern (LBP) histogram features in the spatial domain and the LEDP histogram features of each direction sub-band in the DTCWT domain. On the other hand, the similarity measurement selects matching distances for different features and combines them in the form of convex linear optimization. Texture image retrieval experiments are conducted in the Corel-1k database (DB1), Brodatz texture database (DB2) and MIT VisTex texture database (DB3), respectively. Experimental results show that, compared with the best existing methods, the approach proposed in this article has achieved better retrieval performance.

INDEX TERMS Texture image retrieval, local descriptor, statistical modeling, feature fusion, similarity measurement.

I. INTRODUCTION

With the development of multimedia technology and the arrival of the digital age, the number of digital images in the Internet database increases exponentially. How to search the required images from various databases becomes an urgent problem. Content-based image retrieval (CBIR) is a technique that uses features which can represent image content to search for images which are similar to query images. Usually, CBIR extracts features from both database images and query images, and selects the image that best matches the query image [1]. In other words, CBIR system mainly includes two essential parts: feature extraction and similarity measurement. The effectiveness of the former mainly depends on how to extract features and what types of features are extracted. The accuracy of the latter is determined by which form of similarity measurement is selected. Both affect the performance of retrieval at the same time. Therefore, how to find a useful image retrieval method has become a hot topic in current research. In the literatures [2]–[4], the researchers made a comprehensive and detailed literature review on CBIR.

The texture is a primary visual feature of the image, and texture image represents a large class of natural images. Texture image analysis has been widely used in image retrieval[5], human identification[6], segmentation of remote sensing images[7], defect classification[8], etc. Texture features, shape features and color features are all important features of texture analysis, which can be applied in different fields, especially in the field of image processing. However, when applied to different image processing tasks, the selected features are different[9], [10]. Texture features are significant

The associate editor coordinating the review of this manuscript and approving it for publication was Wenming Cao.

features in image retrieval. Compared with shape and color features, texture features can obtain more image feature information and be effectively extracted in spatial and transform domains. In the transform domain, the statistical features based on wavelet transform have become one of the essential features to describe texture image because wavelet analysis is very consistent with human visual perception. Do *et al*. [11] proposed generalized Gaussian distribution (GGD) statistical features based on detail sub-band coefficients in the discrete wavelet transform (DWT) domain. Kwitt *et al*. [12] proposed the statistical features of Gamma distribution and Weibull distribution of magnitude sub-band coefficients based on DTCWT; Oulhaj *et al*. [13] proposed GGD statistical features of RM sub-band coefficients and Gaussian mixture statistical features of RP sub-band coefficients based on complex wavelet transform [14]. Vo *et al*. [15] used the GGD statistical feature of real and imaginary sub-band coefficients and the Vonn distribution statistical features of RP sub-band coefficients in uniform discrete curvelet complex transform domain. On the other hand, the local pattern feature is a critical feature of texture image in the spatial domain. It is widely used in the classification and retrieval of natural and texture images. Ojala *et al*. [16] proposed LBP and applied it to texture image classification. Zhang *et al*. [17] proposed the local derivative pattern (LDP) for face recognition. Tang *et al*. [18] further extended LBP to face recognition under different illumination conditions. Tajeripour *et al*. [19] proposed a modified LBP for stone porosity computing. Verma *et al*. [20] proposed a local tri-directional pattern (LTriDP) for texture image retrieval. Pan *et al*. [21] proposed local vector quantization pattern(LVQP) for texture classification. Gupta *et al*. [22] proposed color texture image retrieval based on LBP and local extrema peak valley pattern (LDPVP), combined with local directional peak valley pattern (LDPEVP) and color feature. Chakraborty *et al*. [23], [24] proposed local gradual hexagon pattern and R-theta local neighborhood pattern for facial image recognition and retrieval. Dubey *et al*. [25] proposed local bit-plane decoded pattern for biomedical image retrieval. Verma *et al.* [26] combined LBP with local neighborhood difference pattern (LNDP) for natural and texture image retrieval. Liu *et al.* [27], [28] proposed binary rotation invariant and noise tolerant(BRINT) and median robust extended local binary pattern(MRELBP) for texture classification, and these two approaches are robust to noise and illumination, etc. In these methods, the global features of the image captured in the transform domain, lack the description of the local information, while the local features applied to the spatial domain, lack the use of the transform domain information. To further explore the application of local pattern features in the transform domain, Qian *et al.* [29] extended the conventional local binary pattern to pyramid transform domain (PLBP) for texture classification. Akoushideh *et al.* [30] further used the multi-level, multi-resolution approach and multi-band (ML + MR + MB) approach on the basis of PLBP to increase the accuracy of classification. Murala *et al*. [31] proposed a local tetra pattern (LTrP) based on the Gabor wavelet transform domain, which produced four directional features and one magnitude feature, and effectively improved the performance of texture image retrieval. Lei *et al*. [32] used the Gabor wavelet transform to verify that image information in the joint spatial domain and transform domain can provide more useful features.

In recent years, because only one feature can not fully describe the image information, multi-feature fusion has become an effective method for texture image classification and retrieval. Yang *et al*. [33] fused statistical features and LBP features based on the DTCWT domain for texture image classification. Ershad *et al*. [34] fused the gray level co-occurrence matrix (GLCM) and the LBP feature for texture classification, and applied K-L divergence and hybrid color LBP to color image classification [35]. Kumar *et al.* [36] fused LBP features in the spatial domain and mean and variance features in the contourlet transform domain for texture image retrieval, and chi-square distance was used for similarity measurement. Zhou *et al*. [37] proposed to fuse the features of the color histogram, local direction pattern and dense SIFT based on bag of feature (BoF), and use the diffusion process to optimize the global matching of the fused multi-feature images, and use L1 distance as a similarity measurement. Nazir *et al*. [38] proposed a fusion method based on color and shape features, where the color moment and the color histogram are selected to represent color features, and invariant moments are adopted for shape features. Naghashi *et al*. [39] combined two spatial features for fusion, in which the LTP was firstly calculated in the image spatial domain, and then the feature vector was obtained by applying the GLCM in the LTP. In [39], the combination of the above two methods retains the strong robustness of LTP and extracts the spatial correlation between adjacent pixels and the spatial information and frequency of adjacent local patterns through GLCM, and L1 distance is also used as a similarity measurement. Because these methods fuse multiple features, the image information can be fully described, and the performance of texture image retrieval or classification can be effectively improved.

Our motivation is to find a local descriptor in the multi-scale and multi-directional transform domain, which is multi-directional and can make full use of the directional information in the sub-band coefficients. In addition, we hope to select the same statistical model for different sub-band coefficient modeling in the transform domain, and at the same time, find a method that can effectively combine multiple features for texture image retrieval. For these reasons, in this article a new texture image retrieval method which fuses global statistical features and local pattern features is proposed based on the spatial domain and DTCWT domain. Firstly, a new local texture descriptor is proposed in the DTCWT domain. It forms the LEDP in eight directions by judging the relationship between pixel intensity values in six directions and central pixel intensity value. Meanwhile,

FIGURE 1. Base image of 2D-DTCWT.

the magnitude LEDP (MLEDP) and phase LEDP (PLEDP), which play an auxiliary role, are proposed.

Then, the wrapped Cauchy (WC) statistical distribution is used to model both the RP and the RM sub-band coefficients in the DTCWT domain. Finally, LBP is extracted as a complementary feature in the spatial domain. The similarity measurement selects the appropriate distance measure for different features, and the similarity measurements corresponding to all features are combined in the form of convex linear optimization. The effectiveness of the proposed LEDP is verified by comparing experiments in DB1 and DB2 image databases. The efficiency and feasibility of texture image retrieval method based on statistical features and local pattern features are evaluated by comparative experiments in DB2 and DB3 image databases.

To sum up, the main contribution of this article is threefold: i) a new local descriptor LEDP is proposed to make better use of the directional sub-band information in DTCWT domain; ii) the same statistical model is used for the RM sub-band coefficient and the RP sub-band coefficient to ensure the unity of the modeling form; iii) an optimized combination of similarity measurements is used to realize better matching between the extracted features and the corresponding similarity measurements.

The rest of this article is organized as follows. Section II introduces the related theory and the detailed calculation steps of the LEDP. Section III presents in detail the features and similarity measures used in this article. Experimental results and discussions are given in Section IV. Section V concludes with the summary of this article and indicates some possible future work

II. RELATED THEORY

A. DTCWT

DTCWT is a multi-scale and multi-directional image complex transform method proposed by Kingsbury [40]. It has two obvious advantages for texture image analysis: good translation invariance and more direction selectivity. In general, six high-frequency complex directional sub-bands ($\pm 15°, \pm 45°, \pm 75°$) and two low-frequency approximate bands can be obtained by 2-D DTCWT decomposition. Fig.1 illustrates the base image of six directional sub-bands in DTCWT domain. The first line represents the real part direction of the complex wavelet, and the second line represents the imaginary part direction of the complex wavelet.

After DTCWT decomposes the image, the complex sub-band coefficients at different scales can be obtained. Since the complex value sub-band coefficient has two parts: the real part coefficient and the imaginary part coefficient, the phase sub-band coefficient p and the magnitude sub-band coefficient m at the spatial position (i, j) can be obtained by the real part coefficient and the imaginary part coefficient. Through the phase sub-band coefficient p and the magnitude sub-band coefficient m, RP sub-band coefficients and RM sub-band coefficients, which are easier to distinguish texture information, can be obtained, and at the spatial position (i, j) in the complex sub-band they are defined as follows

$$RP\,(i,j) = p_{s,k}\,(i,j) - p_{s,k}\,(i,j+1) \tag{1}$$

$$RM\,(i,j) = m_{s,k}\,(i,j) - m_{s,k}\,(i,j+1) \tag{2}$$

where $RP\,(i,j)$ and $RM\,(i,j)$ represent the RP sub-band coefficient and RM sub-band coefficient at the position (i, j), respectively; $p_{s,k}$ and $m_{s,k}$ represent the phase and magnitude coefficients in the kth direction sub-band at scale s, respectively. The phase sub-band coefficient histogram is uniform and will not produce any distinguishable information about the image, while the RP sub-band coefficient histogram will produce information to distinguish different images [15]. The magnitude sub-band coefficient is always greater than zero, which limits the range of histogram fitting of the selected statistical model. Therefore, RM sub-band coefficient is selected to increase the optional range of statistical model.

B. WRAPPED CAUCHY DISTRIBUTION

The definition of probability density function of wrapped Cauchy distribution can be expressed by (3) as [41]

$$p\,(\theta;\rho,\mu) = \frac{1}{2\pi}\frac{1-\rho^2}{1+\rho^2-2\rho\cos\,(\theta-\mu)} \tag{3}$$

where $\theta \in [-\pi, \pi]$; $\mu \in [-\pi, \pi]$ is the position parameter; $\rho \in [0, 1)$ is the scale parameter, and the larger the value, the sharper the corresponding probability density curve. The model parameters can be estimated by the maximum likelihood method.

C. LBP

Ojala *et al.* [16] proposed LBP for texture image analysis. Given one center pixel of the image, the LBP value can be obtained by comparing the gray value of the center pixel and the gray value of the neighboring pixels. LBP with radius R and neighborhood P is defined as follows

$$LBP_{P,R} = \sum_{p=1}^{P} 2^{(p-1)} \times f_1\left(g_p - g_c\right) \tag{4}$$

$$f_1\,(x) = \begin{cases} 1 & x \geq 0 \\ 0 & \text{else} \end{cases} \tag{5}$$

where g_c is the gray value of the central pixel and g_p is the gray value of the neighboring pixels.

D. LEDP

The LTrP proposed by Murala *et al.* [31] is based on the direction of the pixel to effectively capture the local information of the image. In the spatial domain, firstly, the first derivative of 0° and 90° directions is calculated to get the central pixel direction, and then the LTrP value in the spatial domain is calculated according to the central pixel direction. Meanwhile, The LTrP based on the Gabor transform is also proposed in reference [31], and it uses the 0° and 90° real sub-band coefficients in the Gabor transform domain to calculate the direction of the center pixel of the sub-band image, thus obtaining the LTrP value in the transform domain.

According to Section II.A, each layer in the DTCWT domain generates six complex sub-bands, and the real and imaginary parts of each sub-band have the same direction. In this article, the LEDP based on the DTCWT domain is proposed, and the LEDP in the transform domain is calculated by using the coefficients of the real and imaginary parts of the six directional sub-bands (±15°, ±45°, ±75°). Precisely, given image I, the first-order derivatives along ±15°, ±45° and ±75° directions are denoted as $\boldsymbol{I}_{\theta}^{1}(g_c)|_{\theta=\pm15^\circ,\pm45^\circ,\pm75^\circ}$, and $\boldsymbol{g}_{\theta}|_{\theta=\pm15^\circ,\pm45^\circ,\pm75}$ denote the neighborhood pixel values of the central pixel in the direction sub-band. Then, it can be written as

$$\begin{aligned} I_{15^\circ}^{1}(g_c) &= I(g_{15^\circ}) - I(g_c), \\ I_{45^\circ}^{1}(g_c) &= I(g_{45^\circ}) - I(g_c), \\ I_{75^\circ}^{1}(g_c) &= I(g_{75^\circ}) - I(g_c) \end{aligned} \tag{6}$$

$$\begin{aligned} I_{-15^\circ}^{1}(g_c) &= I(g_{-15^\circ}) - I(g_c), \\ I_{-45^\circ}^{1}(g_c) &= I(g_{-45^\circ}) - I(g_c), \\ I_{-75^\circ}^{1}(g_c) &= I(g_{-75^\circ}) - I(g_c) \end{aligned} \tag{7}$$

and $Dir_{\pm15^\circ}$, $Dir_{\pm45}^{\circ}$ and $Dir_{\pm75^\circ}$ can be calculated by the following formula

$$Dir_{\pm15^\circ} = \begin{cases} 1 & (I_{15^\circ}^{1}(g_c) \geq 0 \text{ and } I_{-15^\circ}^{1}(g_c) \geq 0) \\ & \text{or } (I_{15^\circ}^{1}(g_c) < 0 \text{ and } I_{-15^\circ}^{1}(g_c) < 0) \\ 0 & (I_{15^\circ}^{1}(g_c) < 0 \text{and } I_{-15^\circ}^{1}(g_c) \geq 0) \\ & \text{or } (I_{15^\circ}^{1}(g_c) \geq 0 \text{ and } I_{-15^\circ}^{1}(g_c) < 0) \end{cases}$$

$$Dir_{\pm45^\circ} = \begin{cases} 1 & (I_{45^\circ}^{1}(g_c) \geq 0 \text{ and } I_{-45^\circ}^{1}(g_c) \geq 0) \\ & \text{or } (I_{45^\circ}^{1}(g_c) < 0 \text{ and } I_{-45^\circ}^{1}(g_c) < 0) \\ 0 & (I_{45^\circ}^{1}(g_c) < 0 \text{ and } I_{-45^\circ}^{1}(g_c) \geq 0) \\ & \text{or } (I_{45^\circ}^{1}(g_c) \geq 0 \text{ and } I_{-45^\circ}^{1}(g_c) < 0) \end{cases}$$

$$Dir_{\pm75^\circ} = \begin{cases} 1 & (I_{75^\circ}^{1}(g_c) \geq 0 \text{and } I_{-75^\circ}^{1}(g_c) \geq 0) \\ & \text{or}(I_{75^\circ}^{1}(g_c) < 0 \text{and} I_{-75^\circ}^{1}(g_c) < 0) \\ 0 & (I_{75^\circ}^{1}(g_c) < 0 \text{and } I_{-75^\circ}^{1}(g_c) \geq 0) \\ & \text{or } (I_{75^\circ}^{1}(g_c) \geq 0 \text{and} I_{-75^\circ}^{1}(g_c) < 0) \end{cases} \tag{8}$$

Finally, the obtained $Dir_{\pm15^\circ}$, $Dir_{\pm45^\circ}$,and $Dir_{\pm75^\circ}$ can be converted into the direction of the central pixel by (9)

$$I_{\text{Dir.}}^{1}(g_c) = Dir_{\theta}|_{\theta=\pm15^\circ,\pm45^\circ,\pm75^\circ} \times 2^p + 1, p = 0, 1, 2 \tag{9}$$

where p is the number of directional pairs. From the above formula, the direction of the central pixel may be $1, 2, \ldots, 8$. In this way, the whole image can be converted into eight values (directions).

If the direction obtained by (9) is "1", then the second-order $LEDP^2(g_c)$ of direction 1 can be defined by the following formula

$$\begin{aligned} &\text{LEDP}^2(g_c) \\ &= \begin{matrix} \{f_2(I_{\text{Dir}}^{1}(g_c), I_{\text{Dir}}^{1}(g_1)), f_2(I_{\text{Dir}}^{1}(g_c), I_{\text{Dir}}^{1}(g_2)), \\ \ldots, f_2(I_{\text{Dir}}^{1}(g_c), I_{\text{Dir}}^{1}(g_P))\} |_{P=8} \end{matrix} \end{aligned} \tag{10}$$

$$\begin{aligned} &f_2\left(I_{\text{Dir}}^{1}(g_c), I_{\text{Dir}}^{1}(g_p)\right) \\ &= \begin{cases} 0 & I_{\text{Dir}}^{1}(g_c) = I_{\text{Dir}}^{1}(g_p) \\ I_{\text{Dir}}^{1}(g_p) & \text{else} \end{cases} \end{aligned} \tag{11}$$

where f_2 is a function to judge the relationship between the direction of the center pixel and the direction of the neighborhood pixel. If the direction of the center pixel is the same as that of the neighborhood pixel, the direction of the assigned neighborhood pixel is 0, and if they are different, the original direction will be maintained.

If the 8-bit local pattern values of the central pixel are obtained by (10) and (11), then the seven binary pattern values of direction 1 can be obtained by the following formula

$$\begin{aligned} &\text{LEDP}^2|_{\text{Direction}=2,3,\ldots,8} \\ &= \sum_{p=1}^{P} 2^{(p-1)} \times f_3\left(\text{LEDP}^2(g_c)\right)|_{\text{Direction}=2,3,\ldots,8} \end{aligned} \tag{12}$$

$$f_3\left(\text{LEDP}^2(g_c)\right)|_{\text{Direction}=\phi} = \begin{cases} 1 & \text{LEDP}^2(g_c) = \phi \\ 0 & \text{else} \end{cases} \tag{13}$$

where $\phi = 2, 3, \ldots, 8$, f_3 is a function that converts neighborhood pixel direction to 0 or 1. Similarly, a total of $56(7\times8)$ binary pattern values can be obtained for the other seven directions.

Guo *et al.* [42] proposed the magnitude LBP using the magnitude component of local difference operators and verified its effectiveness. According to their theory, this article puts forward MLEDP and PLEDP. Use the first derivative of the central pixel g_c in the direction of ±15°, ±45°, ±75°, they are as shown in the following formula.

$$\begin{aligned} &M_{I_{\pm15^\circ,\pm45^\circ,\pm75^\circ}^{1}}(g_p) \\ &= \sqrt{\left(I_{15^\circ,45^\circ,75^\circ}^{1}(g_p)\right)^2 + \left(I_{-15^\circ,-45^\circ,-75^\circ}^{1}(g_p)\right)^2} \end{aligned} \tag{14}$$

$$\begin{aligned} &\text{MLEDP} \\ &= \sum_{p=1}^{P} 2^{(p-1)} \times f_1\left(M_{I_{\theta}^{1}(g_p)} - M_{I_{\theta}^{1}(g_c)}\right)|_{P=8,\theta=\pm15^\circ,\pm45^\circ,\pm75^\circ} \end{aligned} \tag{15}$$

$$P_{I^1_{\pm15^\circ,\pm45^\circ,\pm75^\circ}}(g_p) = \arctan\left(\frac{I^1_{15^\circ,45^\circ,75^\circ}(g_p)}{I^1_{-15^\circ,-45^\circ,-75^\circ}(g_p)}\right) \tag{16}$$

$$\text{PLEDP} = \sum_{p=1}^{P} 2^{(p-1)} \times f_1\left(M_{I^1_\theta(g_p)} - M_{I^1_\theta(g_c)}\right)|_{P=8,\theta=\pm15^\circ,\pm45^\circ,\pm75^\circ} \tag{17}$$

where $M_{I^1}(g_p)$ is the magnitude of the pixel, and $P_{I^1}(g_p)$ is the phase of the pixel. In order to reduce the computational complexity, this article selects the uniform patterns [43]. Therefore, for the neighborhood $P = 8$, the feature vector length of the LEDP in each direction is reduced to $P(P-1)+3$.

For a given image I, m scale decompositions are performed in the DTCWT domain to obtain six complex directional sub-bands in each scale. Firstly, the first derivatives of the real and imaginary sub-band coefficients in

each direction are calculated, and then the second-order LEDP(DTLEDP) at six scales can be obtained as follows

$$DT^2_{m,\theta_1}(g_c) = DT^1_{m,\theta_1}(g_c) - DT^1_{m,\theta_1}(g_{45^\circ})|_{\theta_1=15^\circ,45^\circ,75^\circ}, \quad m = 1, 2, .., 6 \tag{18}$$

$$DT^2_{m,\theta_2}(g_c) = DT^1_{m,\theta_2}(g_c) - DT^1_{m,\theta_2}(g_{-45^\circ})|_{\theta_2=-15^\circ,-45^\circ,-75^\circ}, \quad m = 1, 2, .., 6 \tag{19}$$

The direction of the center pixel g_c is calculated by replacing $I^1_{\theta_1}(g_c) \Rightarrow DT^2_{m,\theta_1}(g_c)$ and $I^1_{\theta_2}(g_c) \Rightarrow DT^2_{m,\theta_2}(g_c)$ in (8). Similarly, DTLEDP, MLEDP, and PLEDP values can be obtained by (8) $\sim$ (19). Finally, each layer will respectively produce 8 DTLEDP values for real part and imaginary part sub-band coefficients, and three direction pairs ($\pm15^\circ$, $\pm45^\circ$, $\pm75^\circ$) in each layer will respectively produce three MLEDP values and three PLEDP values for real part and imaginary part sub-band coefficients. Therefore, the 28 (8+8+6+6) local pattern values obtained in each layer are converted into histograms as features.

In order to find the pixel values in the direction of $\pm15^\circ$, $\pm45^\circ$, $\pm75^\circ$, we can draw on the Radon transform idea which can detect the pixel position in any angle of the image [44]. Template images for determining $\pm15^\circ$, $\pm45^\circ$, $\pm75^\circ$ direction pixel value in 11 $\times$ 11 neighborhoods are shown in Fig.2.

Fig. 2 illustrates the pixel values in the direction of $\pm15^\circ$, $\pm45^\circ$, $\pm75^\circ$ and in the neighborhood of $P = 8$, $P = 24$. Considering the amount of calculation and application, only the pixel values in the range of $-90^\circ \sim 90^\circ$ are selected for neighborhood pixel values, as shown in Fig. 3.

Fig. 3 illustrates that, the yellow area is the neighborhood pixel of g_c with $R = 1$, and the blue area is the neighborhood pixel of g_c with $R = 2$. In this article, the neighborhood pixels of $R = 1$ are selected to calculate LEDP. With the increase of the radius, the direction may also increase, that is, the number of features will increase. In the future work, we will continue to use the neighborhood pixels of $R = 2$ to calculate the third-order LEDP.

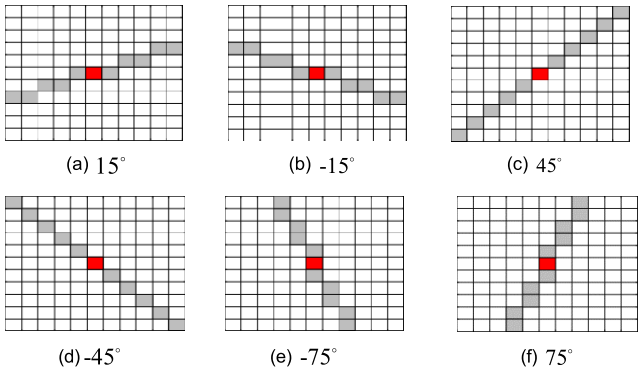

FIGURE 2. Template images of ±15°, ±45°, ±75° direction pixel value in 11 × 11 neighborhoods.

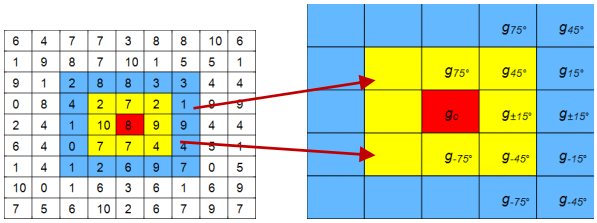

FIGURE 3. Neighborhood pixel of g_c with $R = 1$ and $R = 2$ in direction of ±15°, ±45°, ±75°.

III. TEXTURE IMAGE RETRIEVAL METHOD

Texture image retrieval includes two essential parts: feature extraction and similarity measurement. The feature extraction part is used to select the features which can fully reflect the image information. The excellent features should reflect the global overview of the image and describe the local image information. The performance of retrieval can be effectively improved by fusing these two features. In this article, we choose the same statistical model (i.e., WC distribution) for RM and RP sub-band coefficient modeling respectively in the DTCWT domain, which can effectively ensure the uniformity of global modeling parameter features and corresponding similarity measurements. To compensate for the loss of local information due to using global features in the transform domain, we propose a new image local descriptor (i.e., LEDP) to extract local features in the DTCWT transform domain, and meanwhile the LBP local feature information in the spatial domain is also used. On the other hand, the matching similarity measurements are selected for the extracted features. K-L divergence is selected as the similarity measurement for the statistical model parameter features, and the relative L1 distance is used as the similarity measurement for both local descriptor features.

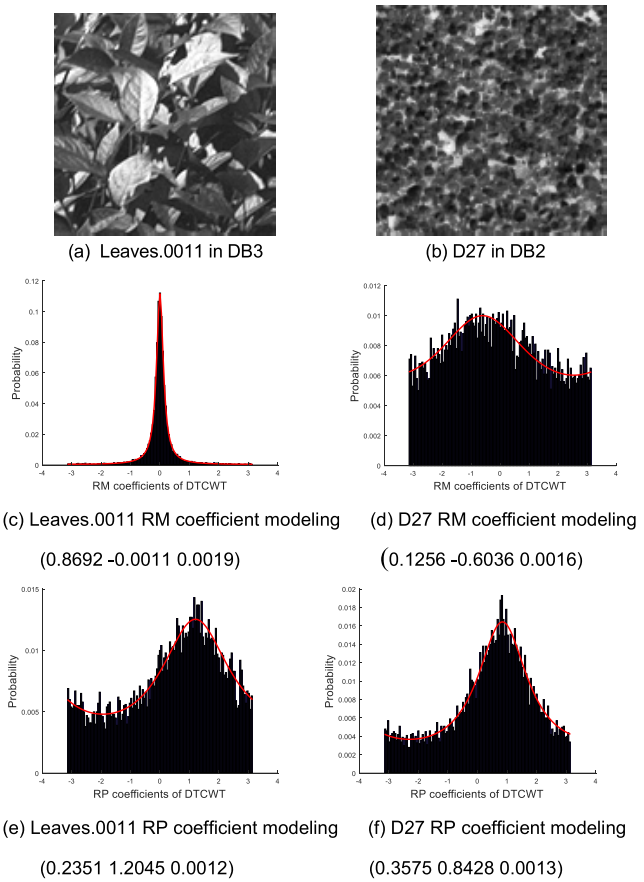

FIGURE 4. Statistical modeling and histogram fitting of database images.

A. SUB-BAND COEFFICIENT MODELING AND GLOBAL FEATURE SELECTION

The global features of texture image are determined by the statistical modeling parameters of directional sub-band coefficients in the DTCWT domain in this article. To unify the modeling form of DTCWT sub-band coefficients, both the RM sub-band coefficient and the RP sub-band coefficient select the WC distribution to model. In order to verify the rationality of the selected statistical model, and considering the limited space, two typical images are selected from each of the DB2 and DB3 databases for DTCWT decomposition. Then the sub-band coefficients of different directions under different scales are modeled. The typical experimental results are shown in Fig. 4. The first row is the images in each image database; The second row is WC distribution modeling and histogram fitting of RM sub-band coefficients with third scale and 15 ° direction; The third row is WC distribution modeling and histogram fitting of RP sub-band coefficients with third scale and 15 ° direction. In the parentheses at the bottom of the fitting figures, the first two numbers are the parameters of the model (ρ, μ), and the last one is the objective evaluation index, namely entropy difference rate R_e. R_e is defined as the ratio of the K-L distance between histogram and model distribution or relative entropy (ΔH) to entropy value (H) of histogram distribution[15], and the smaller the value, the better the fit.

TABLE 1. Comparison of Distance Within Class and Distance Between Classes.

	Two models		One model	
Image modeling	RP-WC	RM-GGD	RP-WC	RM-WC
Distance within class	29.26	0.89	29.26	4.4826
Distance between classes	13.82	4.9279	13.82	24.38
Comparison	29.26+0.89>13.82+4.9219		29.26+4.4826<13.82+24.38	

Fig.4 illustrates the fitting effect of each histogram and the size of R_e, which can be seen that the selected statistical model can well fit the histogram of sub-band coefficients, that is, the coefficient modeling is suitable for RM and RP sub-bands. We observe that the model parameter values of different classes of texture images are different, therefore the differences between different texture images can be effectively distinguished by the model parameter features.

More importantly, this can alleviate the problem that the distance within the classes is greater than the distance between classes using different statistical models. To verify the advantages of this modeling scheme, the 631st and 640th images in the DB3 image database (both belong to the same class of image), and the 475th and 640th images (both belong to different classes of images) in the DB3 image database are selected to model and estimate the model parameters, and the K-L distance within the classes and the K-L distance between the classes are respectively calculated, and the results are shown in Table 1.

The data from Table 1 show that the distance within the class is larger than the distance between classes when the RP and RM sub-band coefficients are respectively modeled by the two models; while the distance within the class is less than the distance between classes when the RP and RM sub-band coefficients are respectively modeled by the same model. Therefore, the selection of the modeling scheme in this article can improve the performance of texture image retrieval.

B. LEDP AND LOCAL FEATURE SELECTION

The local features in this article are mainly obtained from the LEDP (also including MLEDP and PLEDP) histogram of directional sub-bands in the DTCWT domain. To verify that the proposed LEDP is multi-directional, we choose to compare it with the same multi-directional LTrP. Select the same test image and apply LTrP and LEDP respectively to obtain four directions of LTrP and eight directions of LEDP. The experimental results are shown in Fig. 5.

Fig.5 illustrates that the selected test images have obvious multiple directionalities, which can be used to distinguish the ability of different local descriptors to describe the direction; compared with LTrP, LEDP can represent more detailed direction information. Therefore, LEDP is easy to capture more local direction feature information for texture images

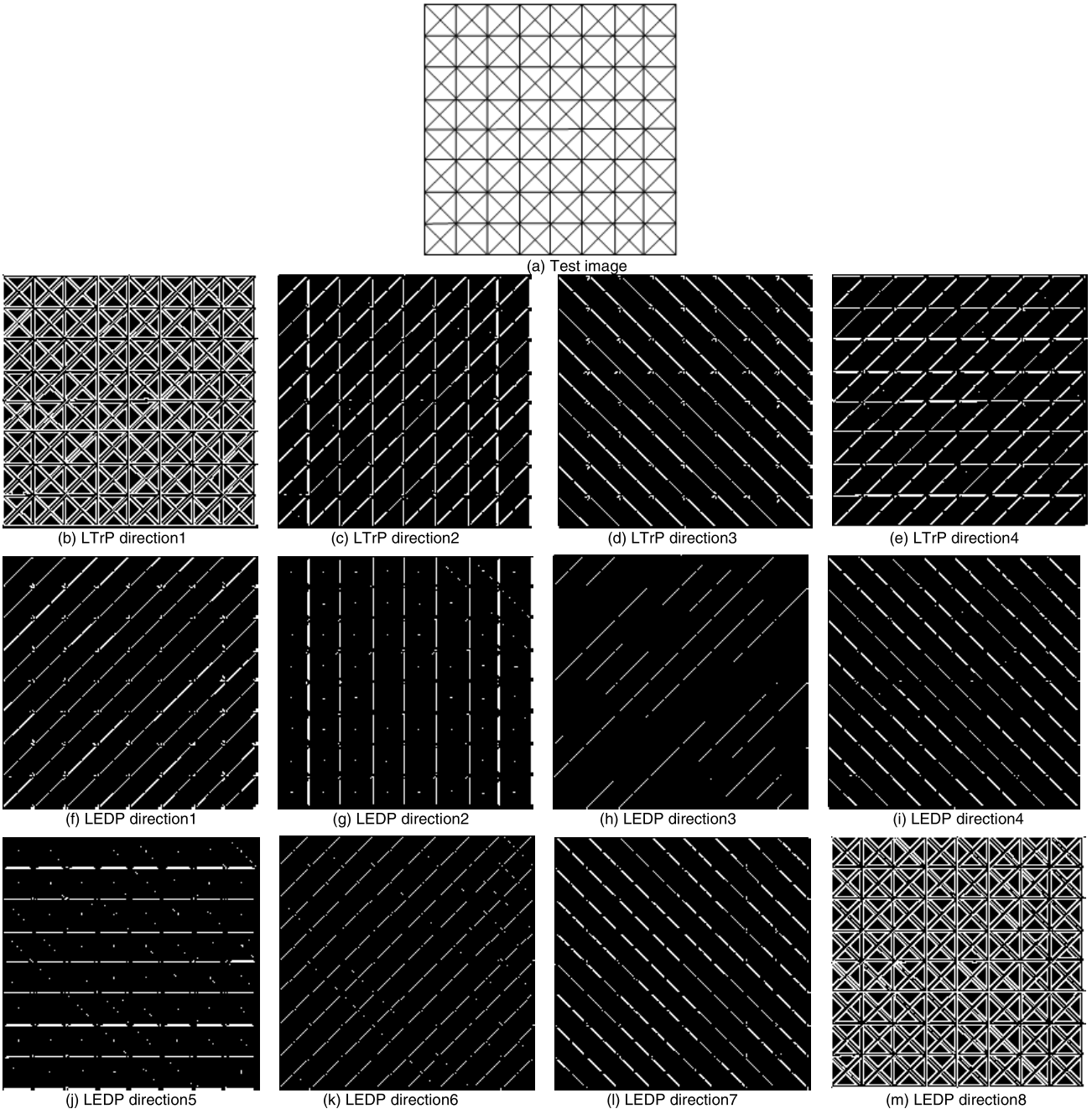

FIGURE 5. **Directional effect comparison of LEDP and LTrP.**

with rich direction information, and can better combine with DTCWT direction sub-bands, thus effectively improve the effect of texture image retrieval.

C. LEDP ROBUSTNESS

The LEDP proposed in this article has many nice properties. In order to verify these, the Tile.0001 image in DB3 database is selected for experiments. We tested the properties of the resistance against rotation, illumination, and scaling of LEDP respectively, and the experimental results are shown in Fig 6. Because there are many directional atlas produced by LEDP, limited to space, only part of the directional spectrum of LEDP (direction 1 and direction 8) are selected for testing. At the same time, because some of the properties can not be seen directly from the LEDP spectrum, the histograms of the eight directional spectrums generated by LEDP are merged.

Our experimental scheme is to verify the robustness of LEDP in the resistance against rotation, illumination, and scaling by comparing LEDP spectrums and LEDP histograms under different conditions. From Fig 6. (e)∼(i), we can see that the LEDP spectrum of the original image under different illumination is basically the same; when the original image is rotated by 90°, the LEDP spectrum obtained is also close to the original image spectrum. From Fig 6 (m)∼(r), we can

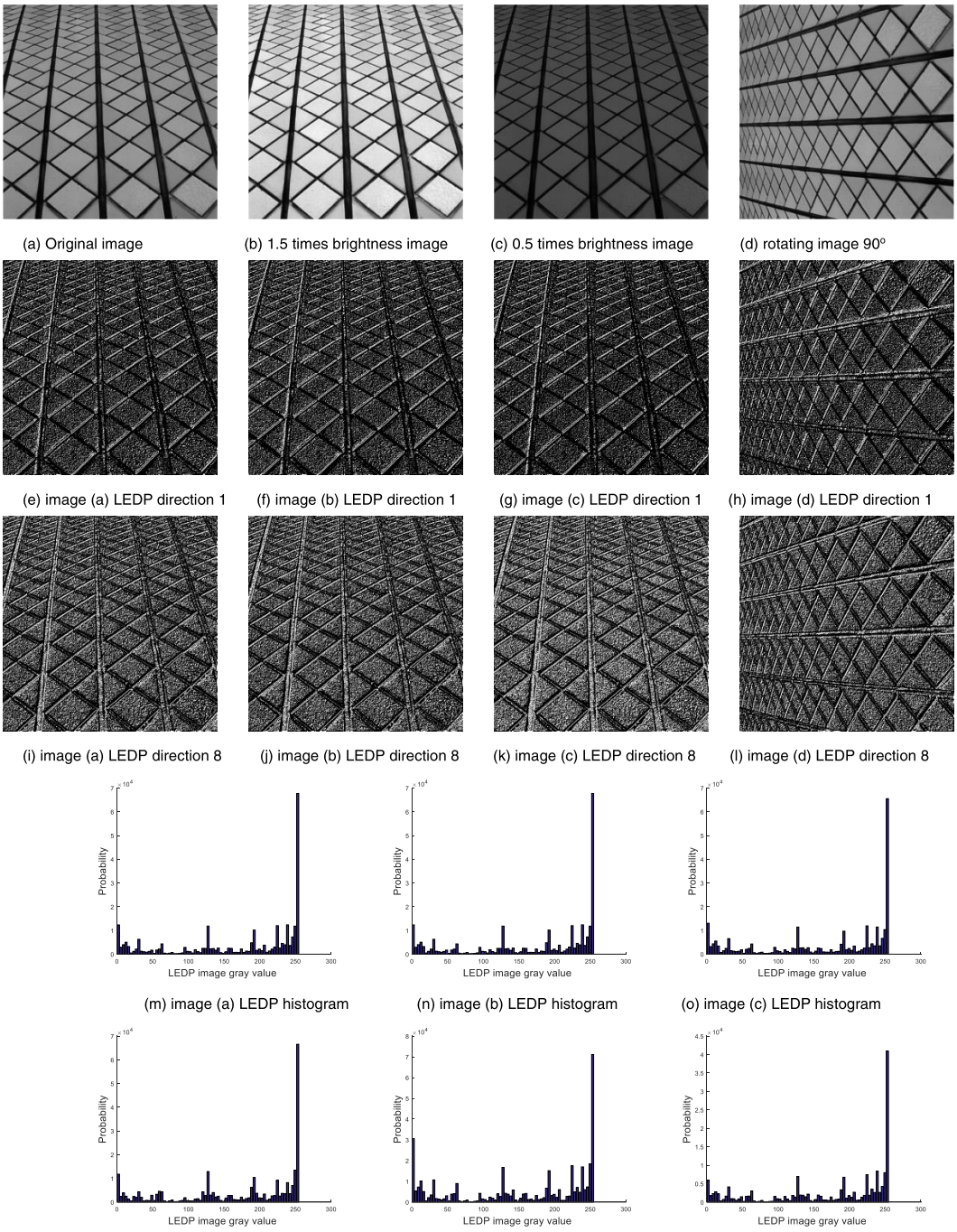

FIGURE 6. Image LEDP direction 1 atlas and direction 8 spectrum and LEDP histogram under different conditions.

see that the shape of LEDP histogram is very similar under different conditions such as illumination, rotation and scaling. In summary, the experimental results

show that the LEDP proposed in this article has good robustness in the resistance against rotation, illumination, and scaling of the texture images.

D. SIMILARITY MEASUREMENT

In this article, K-L divergence is used to similarity measurement corresponding to the parameter features of the WC statistical distribution model. However, because this similarity measurement does not have a closed-form, it can be estimated by the numerical method [15]. For each direction sub-band in DTCWT domain, the used K-L divergence is defined as

$$D_C\left(p\left(\theta;\rho_1,\mu_1\right),q\left(\theta;\rho_2,\mu_2\right)\right) = \int_{-\pi}^{\pi} p\left(\theta;\rho_1,\mu_1\right)\ln\frac{p\left(\theta;\rho_1,\mu_1\right)}{q\left(\theta;\rho_2,\mu_2\right)}d\theta \quad (20)$$

where $p\left(\theta;\rho_1,\mu_1\right)$ and $q\left(\theta;\rho_2,\mu_2\right)$ are respectively WC probability density functions of database candidate images

and query images;ρ_1, μ_1 and ρ_2, μ_2 denote the scale and location parameters of the statistical model of database candidate image and query image, respectively. Correspondingly, the similarity measurement between each sub-band statistical model of RM and RP is expressed as D_{RM} and D_{RP}, respectively.

The relative L1 distance is chosen as the similarity measurement corresponding to the histogram features of LBP and LEDP local descriptors. At the same time, the normalized Euclidean distance (L2) is selected as the comparative experiment for the similarity measurement. For each bin of the histogram, the relative L1 distance and L2 are respectively defined as

$$D_{L_1}(A, B) = \left| \frac{h_{l1,i} - h_{l2,i}}{1 + h_{l1,i} + h_{l1,i}} \right| \tag{21}$$

$$D_{L_2}(A, B) = \frac{\left| h_{l1,i} - h_{l2,i} \right|}{M} \tag{22}$$

where $h_{l1,i}$ and $h_{l2,i}$ denote the histogram features of the database candidate images and the query images, respectively, and i is the ith bin of the feature histogram, M is the standard deviation of all bin values. Correspondingly, for each bin, the similarity measurement of LBP is denoted as D_{LBP}; and for each sub-band and each bin, the similarity measurement of LEDP is expressed as D_{LTrP}.

Finally, the similarity measurements corresponding to various features are combined into a total similarity

measurement in the form of a convex linear combination. It is defined as

$$D = a \sum_{m=1}^{M} D_{RM} + b \sum_{m=1}^{M} D_{RP} + c \sum_{k=1}^{K_1} D_{LBP} + d \sum_{n=1}^{N} \sum_{k=1}^{K_2} D_{LEDP} \tag{23}$$

where M and N are the numbers of directional sub-bands, K_1 and K_2 are the numbers of bins in histogram, and $a + b + c + d = 1, 0 \leq a, b, c, d \leq 1$.In the experiment, using the retrieval method proposed in this article, through MATLAB simulation, traversing the numerical range of a, b and c with the iteration step size 0.001, and according to the optimal average retrieval rate, $a = 0.018$, $b = 0.072$, $c = 0.82$, and $d = 0.09$ are set in the DB2 image database; $a = 0.02$, $b = 0.08$, $c = 0.8$, and $d = 0.1$ are set in the DB3 image database.

E. PROPOSED METHOD

The retrieval algorithm proposed in this article is shown as follows

Algorithm

Input: *Query image;* **Output:** *Retrieval result*

1: Load the image and convert it to a grayscale image.
2: Calculate the LBP value of the image in the spatial domain, and establish the feature histogram.
3: Decompose the image by DTCWT, and calculate the RM and RP sub-band coefficients.
4: Model the WC distribution of RM and RP sub-band coefficients.
5: Calculate the LEDP value, MLEDP value, and PLEDP value of the image in DTCWT domain, and establish the feature histogram.
6: Construct the feature vector.
7: Compare the query image with the image in the image database using (23).
8: Retrieve the most matching N images.

IV. EXPERIMENTS AND DISCUSSION

In order to present and compare the performance of the method proposed in this article, three widely used texture image databases are selected for the experiments. The following comparative experiments are conducted to verify the effectiveness of this method by setting different database combinations.

A. EXPERIMENTAL DATABASES

All retrieval experiments in this article are carried out in three texture image databases. The first image database used images from the Corel database [45]. Some researchers think that the Corel database meets all the requirements to evaluate an image retrieval system due to its large size and heterogeneous content. In the experiment, 1000 images were collected and divided into ten categories to form the large-sized database DB1. These images come from ten different types of domains, namely, *Africans, beaches, buildings, buses, dinosaurs, elephants, flowers, horses, mountains,* and *food.* Each category has 100 images with resolution of either 256 × 384 or 384 × 256. The second image database contains 116 different categories of texture images with resolution of 512 × 512, of which 109 texture images are from Brodatz texture image database [46] and seven texture images are from the University of Southern California image database [47]. Each image with resolution of 512 × 512 is divided into 16 non-overlapping sub-images with resolution of 128 × 128, thus creating the medium-sized image database DB2 with 116 categories, 16 images per category, and a total of 1856 (116 × 16) images. The third image database contains 40 different types of texture images with resolution of 512 × 512, all of which come from the MIT VisTex texture image database [48]. Each image with resolution of 512 × 512 is also divided into 16 non-overlapping sub-images with resolution of 128 × 128, thus creating the small-sized image database DB3 with a total of 640 (40 × 16) images, 40 categories and 16 images per category. Fig.7 illustrates sample images of three image databases. Besides, for DB2 and DB3 image databases, to reduce the correlation of gray values among similar sub-images and maintain the fairness of the retrieval process, all sub-category images are respectively normalized to zero mean and unit standard deviation.

B. PERFORMANCE EVALUATION INDEX

In the experiments, each image in the image database is treated as a query image. According to the extracted image

FIGURE 7. Some samples of gray-scale textures in the three image databases:(top) DB1, (middle) DB2, (bottom) DB3.

features, the similarity measurement is calculated by (23), and finally, the top N images with the shortest distance from the query image are selected in the database. The performance of the retrieval system in this article is respectively evaluated by precision, recall and average retrieval rate (ARR), which are defined as

$$Precison = \frac{\sum_{i=1}^{M} s_i}{V} \tag{24}$$

$$Recall = \frac{\sum_{i=1}^{M} s_i}{R} \tag{25}$$

$$ARR = \frac{\sum_{i=1}^{M} s_i}{MV}\Big|_{V=16} \tag{26}$$

where M is the total number of images in the database, S_i is the number of correct images retrieved for the ith time, V is the number of images retrieved each time, and R is the number of images of each category.

C. COMPARISON OF RETRIEVAL PERFORMANCE BASED ON LTRP AND LEDP IN DB1 AND DB2

In order to compare the effect of two local direction descriptors, namely LTrP and LEDP proposed in this article, on the performance of texture image retrieval, the experiments are carried out in two distinct image databases DB1 and DB2. The experimental results are shown in Fig.8 and Table 2. Fig.8 illustrates the comparisons of the precision and the recall between LEDP and LTrP based on the spatial domain and the transform domain in the ten categories of images from the DB1 image database.

Given below are the abbreviations used in the analysis of the experimental results.

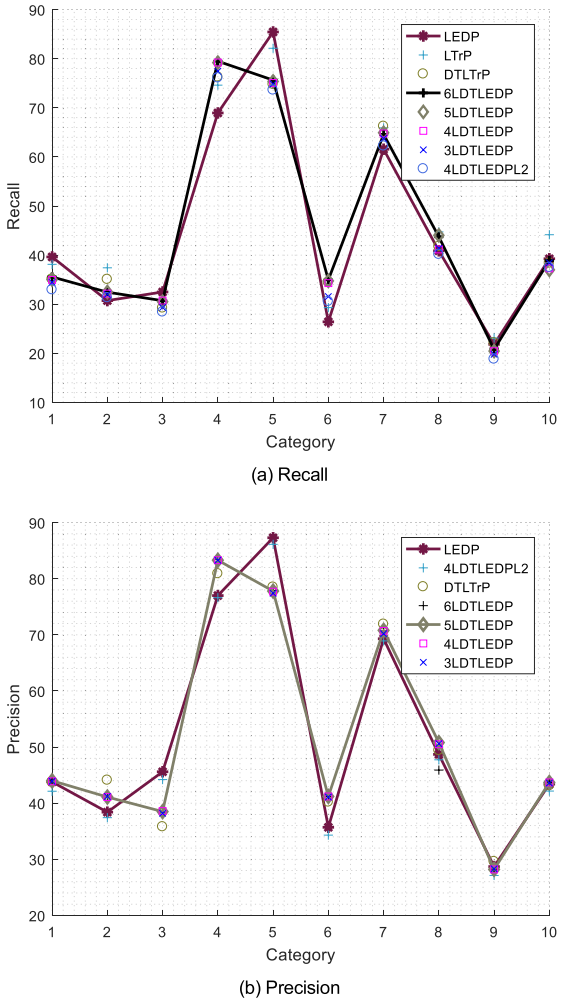

FIGURE 8. Comparison of precision and recall results for 10 categories of images.

LBP: LBP features[31]
DTLBP: LBP in DTCWT
LDP: Local derivative patterns [17]
LTP: Local ternary patterns [18]
LTrP: Local tetra patterns [31]
GLTrP: Local tetra patterns with GT [31]
LMEBP: Local maximum edge patterns [49]
DTLTrP: LTrP in DTCWT
LEDP: Local eight direction patterns
3-6 LDTLEDP: Local eight direction patterns with three-six layer decompositions in DTCWT
4 LDTLEDPL2: Local eight direction patterns with four layer decompositions in DTCWT with L2 distance

Fig.8(a) illustrates that, in the spatial domain, the recall of LEDP in 3 out of 10 categories is better than that of LTrP for the DB1 image database; in the transform domain, the recall of 7 out of 10 categories of DTLEDP is better than that of DTLTrP. These results show that the local descriptor LEDP proposed in this article has more advantages in the DTCWT domain over LTrP. Fig.8(b) illustrates that, compared with DTLTrP, DTLEDP has similar advantages in

TABLE 2. ARR Comparisons for Different Descriptors in DB2.

Method	ARR (%)
LBP [31]	79.97
DTLBP	76.35
LDP [17]	78.70
LTP [18]	79.96
LTrP [31]	85.30
GLTrP [31]	82.04
LMEBP [49]	83.28
DTLTrP	81.25
LEDP	83.52
3LDTLEDP	82.68
4LDTLEDP	82.74
4LDTLEDPL2	81.42
5LDTLEDP	82.71
6LDTLEDP	82.65

precision, where 6 out of 10 categories of DTLEDP have better precision than DTLTrP. When the similarity measurement is L2, the precision and recall are lower than that of L1, which proves the rationality of the similarity measurement selected in this article. Besides, setting different decomposition layers in DTCWT domain also affects the retrieval performance of DTLEDP. When the number of decomposition layers is appropriately increased, the retrieval performance will be improved. However, when the number of decomposition layers is increased to some extent, the retrieval performance will decrease instead. For this reason, in order to ensure better retrieval performance, we selects 5-layer decompositions for DTLEDP in this article.

Table.2 shows that, for the DB2 image database, LEDP and DTLEDP are used to compare the ARR with other existing local descriptors.

From the data in Table.2, we can show that, the retrieval performances of LEDP and DTLEDP are superior to most existing local descriptors on image database DB2. Nevertheless, their retrieval performance is still lower, compared with that of LTrP. This result may be caused by the fact that some of the eight directions of LEDP are not sensitive to random information of a few images. Considering that the LEDP proposed in this article is mainly applied to the DTCWT domain, and in order to better utilize the direction information of the sub-bands, compared with DTLBP, GLTrP and DTLTrP, DTLEDP indeed has certain advantages. Therefore, DTLEDP can provide more local direction information than DTLTrP in DTCWT domain.

TABLE 3. ARR for DB2 and DB3 Image Database.

Method	ARR (%)	ARR (%)
	DB2	DB3
GGD-WC [34]	-	85.64
GGD-Vonn [14]	-	85.82
LBP [31]	79.97	82.30
LMEBP [49]	83.28	87.77
SVD+LBP [50]	83.01	88.56
CoALTP [39]	77.94	86.53
LDPVBP-CH [22]	-	85.00
LTriDP [20]	76.45	88.62
LNDP+LBP [26]	76.41	-
DTLEDP	82.74	87.01
RM	72.45	82.45
LBP+DP	83.22	88.01
LBP+RM	82.22	87.56
RM+DP	83.23	87.44
PM_{L2}	83.45	88.23
$PM_{N=25}$	79.94	-
PM	**84.04**	**89.11**

D. COMPARE RETRIEVAL PERFORMANCE OF DIFFERENT METHODS IN DB2 AND DB3

Select some existing methods which use image database DB2 and DB3 to compare the retrieval performance (ARR) with the method proposed in this article, and the experimental results are shown in Table 3. In Table 3, the "GGD-WC" and "GGD-Vonn" methods use the GGD distribution parameter features of the sub-band coefficients, and the WC distribution parameter features and the Vonn distribution parameter features of the RP sub-band coefficients in the uniformly discrete curvelet complex transform domain [15], [41]; the "LBP", "LMEBP" and "LTriDP" methods use the histogram features of LBP, LMEBP and LTriDP in spatial domain [20], [31], [49]; the "SVD+LBP" method combines the singular value decomposition (SVD) feature in the DTCWT domain with the LBP histogram feature in the spatial domain[50]; the "CoALTP" method fuses LTP and GLCM in spatial domain[39]; the "LDPVBP-CH" method fuses LDPVBP and CH in spatial domain [22]; the "LNDP+LBP" method fuses LNDP and LBP in spatial domain [26]; The "RM" method uses only the statistical features of WC distribution in DTCWT domain; the "LBP+DP" method uses LBP in spatial domain and DTLEDP in DTCWT domain; the "LBP+RM" method uses

TABLE 4. Feature Vector Length and ARR in DB2 for PM and Prior Methods.

Method	Feature Vector Length	ARR (%)
LBP [31]	59	79.97
LDP [17]	144	78.07
LTP [18]	72	79.96
LEDP	826	**83.52**
GLTrP [31]	2301	82.04
DTLEDP	6490	82.74
DTLTrP	5310	81.25
LMEBP [49]	4096	83.28
SVD+LBP [50]	114	83.01
CoALTP [39]	2048	77.94
LTriDP [20]	768	76.45
LNDP+LBP [26]	512	76.41
RM	72	72.45
LBP+DP	6549	83.22
LBP+RM	131	82.22
RM+DP	6562	83.23
PM	6621	**84.04**

LBP in spatial domain and statistical features of WC distribution in DTCWT domain; the ''RM+DP'' method uses statistical features of WC distribution and DTLEDP in DTCWT domain. It should be noted that the texture images of the DB2 image database used by the ''LNDP+LBP'' and ''LTriDP'' methods are all from the Brodatz texture image database with a total of 2800 (112×25) texture images. In addition, ''PM'' is the method proposed in this article in Table 3. In our retrieval experiments, from the perspective of obtaining the best average retrieval rate, three layer decompositions in DTCWT domain are used for extracting the statistical modeling features; and five layer decompositions in DTCWT domain are used for extracting DTLEDP and MLEDP and PLEDP features; and the number of the bin is 59 for all local pattern histogram.

From the data in Table.3, it can be seen that the retrieval performance achieved by the method proposed in this article is better than the best results of existing approaches, which shows that our method is effective. Besides, compared with the ARR obtained respectively by the ''LBP+DP'', ''LBP+RM'' and ''RM+DP'' methods, the three feature fusion method exploited in this article substantially improve the ability to characterize texture images.

E. FEATURE VECTOR LENGTH AND PERFORMANCE

Table 4 shows feature vector length and ARR in DB2 for PM and prior methods. We can see that from Table 4, although the feature vector length of PM is higher than that of other methods, its retrieval performance outperforms others in terms of ARR.

V. CONCLUSION

In image retrieval, the use of multi-feature fusion can effectively enhance the ability of feature representation of images, thus significantly improve retrieval performance. For this reason, a new method of texture image retrieval is proposed in this article based on the DTCWT domain and spatial domain, which combines global statistical features and local pattern features. Specifically, this method combines the LEDP features proposed in this article, LBP features and statistical features to characterize the texture information of the image. Accordingly, the similarity measurement uses a convex linear optimization form, which combines the similarity measurements corresponding to each feature. The results of the retrieval experiments in Corel (DB1), Brodatz (DB2) and VisTex (DB3) image databases verify the effectiveness and feasibility of our method; and compared with the best results of existing methods, the proposed approach has obvious advantages in the retrieval performance.

In this article, the LEDP is only applied to the DTCWT domain. In addition, it can also be applied to pyramid dual tree directional filter bank (PDTDFB) and Gabor complex transform domains with more flexible directionality. On the other hand, only relative magnitude sub-bands and relative phase sub-bands in DTCWT domain are modeled, but the low frequency sub-bands in the DTCWT domain are not exploited to model. In the future, we will continue to look for statistical models suitable for all DTCWT sub-bands to improve retrieval performance. Furthermore, because of the effectiveness of the method proposed in this article, it can also be applied to the retrieval of other image databases, such as facial image and biomedical image databases.

REFERENCES

[1] F. Tajeripour, M. Saberi, and S. F. Ershad, ''Developing a novel approach for content based image retrieval using modified local binary patterns and morphological transform,'' *Int. Arab J. Inf. Technol.*, vol. 12, no. 6, pp. 574–581, 2015.
[2] M. M. B. Ismail, ''A survey on content based image retrieval,'' *Int. J. Adv. Comput. Sci. Appl.*, vol. 8, no. 5, pp. 159–170, 2017.
[3] A. Latif, A. Rasheed, U. Sajid, J. Ahmed, N. Ali, N. I. Ratyal, B. Zafar, S. H. Dar, M. Sajid, and T. Khalil, ''Content-based image retrieval and feature extraction: A comprehensive review,'' *Math. Problems Eng.*, vol. 2019, Aug. 2019, Art. no. 9658350.
[4] F. Rajam and S. Valli, ''A survey on content based image retrieval,'' *Life Sci. J.*, vol. 10, no. 2, pp. 2475–2487, 2013.
[5] M. A. Belarbi, S. Mahmoudi, and G. Belalem, ''PCA as dimensionality reduction for large-scale image retrieval systems,'' *Int. J. Ambient Comput. Intell.*, vol. 8, no. 4, pp. 45–58, Oct. 2017.
[6] S. Angadi and S. Nandyal, ''Human identification system based on spatial and temporal features in the video surveillance system,'' *Int. J. Ambient Comput. Intell.*, vol. 11, no. 3, pp. 1–21, Jul. 2020.
[7] S. Hemalatha and S. M. Anouncia, ''Unsupervised segmentation of remote sensing images using FD based texture analysis model and ISODATA,'' *Int. J. Ambient Comput. Intell.*, vol. 8, no. 3, pp. 58–75, Jul. 2017.

[8] Q. Luo, Y. Sun, P. Li, O. Simpson, L. Tian, and Y. He, "Generalized completed local binary patterns for time-efficient steel surface defect classification," *IEEE Trans. Instrum. Meas.*, vol. 68, no. 3, pp. 667–679, Mar. 2019.

[9] J. Chaki, and N. Dey, *A Beginner's Guide to Image Shape Feature Extraction Techniques*. Boca Raton, FL, USA: CRC Press, 2019.

[10] J. Chaki, and N. Dey, *Texture Feature Extraction Techniques for Image Recognition*. Singapore: Springer, 2020.

[11] M. N. Do and M. Vetterli, "Wavelet-based texture retrieval using generalized Gaussian density and Kullback-Leibler distance," *IEEE Trans. Image Process.*, vol. 11, no. 2, pp. 146–158, 2002.

[12] R. Kwitt and A. Uhl, "Lightweight probabilistic texture retrieval," *IEEE Trans. Image Process.*, vol. 19, no. 1, pp. 241–253, Jan. 2010.

[13] H. Oulhaj, R. Jennane, A. Amine, M. El Hassouni, and M. Rziza, "Study of the relative magnitude in the wavelet domain for texture characterization," *Signal, Image Video Process.*, vol. 12, no. 7, pp. 1403–1410, Oct. 2018.

[14] H. Oulhaj, M. Rziza, A. Amine, R. Jennane, and M. El Hassouni, "Texture classification using relative phase and Gaussian mixture models in the complex wavelet domain," in *Proc. IEEE/ACS 13th Int. Conf. Comput. Syst. Appl.*, Nov. 2016, pp. 1–7.

[15] A. Vo, S. Oraintara, and N. Nguyen, "Vonn distribution of relative phase for statistical image modeling in complex wavelet domain," *Signal Process.*, vol. 91, no. 1, pp. 114–125, Jan. 2011.

[16] T. Ojala, M. Pietikäinen, and D. Harwood, "A comparative study of texture measures with classification based on featured distributions," *Pattern Recognit.*, vol. 29, no. 1, pp. 51–59, Jan. 1996.

[17] B. Zhang, Y. Gao, S. Zhao, and J. Liu, "Local derivative pattern versus local binary pattern: Face recognition with high-order local pattern descriptor," *IEEE Trans. Image Process.*, vol. 19, no. 2, pp. 533–544, Feb. 2010.

[18] X. Tan and B. Triggs, "Enhanced local texture feature sets for face recognition under difficult lighting conditions," *IEEE Trans. Image Process.*, vol. 19, no. 6, pp. 1635–1650, Jun. 2010.

[19] F. Tajeripour and S. Fekri-Ershad, "Developing a novel approach for stone porosity computing using modified local binary patterns and single scale retinex," *Arabian J. Sci. Eng.*, vol. 39, no. 2, pp. 875–889, Feb. 2014.

[20] M. Verma and B. Raman, "Local tri-directional patterns: A new texture feature descriptor for image retrieval," *Digit. Signal Process.*, vol. 51, pp. 62–72, Apr. 2016.

[21] Z. Pan, H. Fan, and L. Zhang, "Texture classification using local pattern based on vector quantization," *IEEE Trans. Image Process.*, vol. 24, no. 12, pp. 5379–5388, Dec. 2015.

[22] S. Gupta, P. P. Roy, D. P. Dogra, and B.-G. Kim, "Retrieval of colour and texture images using local directional peak valley binary pattern," *Pattern Anal. Appl.*, vol. 23, pp. 1–17, Apr. 2020.

[23] S. Chakraborty, S. K. Singh, and P. Chakraborty, "Local gradient hexa pattern: A descriptor for face recognition and retrieval," *IEEE Trans. Circuits Syst. Video Technol.*, vol. 28, no. 1, pp. 171–180, Jan. 2018.

[24] S. Chakraborty, S. K. Singh, and P. Chakraborty, "R-theta local neighborhood pattern for unconstrained facial image recognition and retrieval," *Multimedia Tools Appl.*, vol. 78, no. 11, pp. 14799–14822, Jun. 2019.

[25] S. R. Dubey, S. K. Singh, and R. K. Singh, "Local bit-plane decoded pattern: A novel feature descriptor for biomedical image retrieval," *IEEE J. Biomed. Health Informat.*, vol. 20, no. 4, pp. 1139–1147, Jul. 2016.

[26] M. Verma and B. Raman, "Local neighborhood difference pattern: A new feature descriptor for natural and texture image retrieval," *Multimedia Tools Appl.*, vol. 77, no. 10, pp. 11843–11866, May 2018.

[27] L. Liu, S. Lao, P. W. Fieguth, Y. Guo, X. Wang, and M. Pietikainen, "Median robust extended local binary pattern for texture classification," *IEEE Trans. Image Process.*, vol. 25, no. 3, pp. 1368–1381, Mar. 2016.

[28] L. Liu, Y. Long, P. W. Fieguth, S. Lao, and G. Zhao, "BRINT: Binary rotation invariant and noise tolerant texture classification," *IEEE Trans. Image Process.*, vol. 23, no. 7, pp. 3071–3084, Jul. 2014.

[29] X. Qian, X.-S. Hua, P. Chen, and L. Ke, "PLBP: An effective local binary patterns texture descriptor with pyramid representation," *Pattern Recognit.*, vol. 44, nos. 10–11, pp. 2502–2515, Oct. 2011.

[30] A. Akoushideh and B. Mazloom-Nezhad Maybodi, "Efficient levels of spatial pyramid representation for local binary patterns," *IET Comput. Vis.*, vol. 9, no. 6, pp. 871–883, Dec. 2015.

[31] S. Murala, R. P. Maheshwari, and R. Balasubramanian, "Local tetra patterns: A new feature descriptor for content-based image retrieval," *IEEE Trans. Image Process.*, vol. 21, no. 5, pp. 2874–2886, May 2012.

[32] Z. Lei, S. Liao, M. Pietikäinen, and S. Z. Li, "Face recognition by exploring information jointly in space, scale and orientation," *IEEE Trans. Image Process.*, vol. 20, no. 1, pp. 247–256, Jan. 2011.

[33] P. Yang and G. Yang, "Statistical model and local binary pattern based texture feature extraction in dual-tree complex wavelet transform domain," *Multidimensional Syst. Signal Process.*, vol. 29, no. 3, pp. 851–865, Jul. 2018.

[34] S. F. Ershad, "Texture classification approach based on combination of edge & co-occurrence and local binary pattern," 2012, *arXiv:1203.4855*. [Online]. Available: http://arxiv.org/abs/1203.4855

[35] S. Fekri-Ershad and F. Tajeripour, "Impulse-noise resistant color-texture classification approach using hybrid color local binary patterns and Kullback–Leibler divergence," *Comput. J.*, vol. 60, no. 11, pp. 1633–1648, Nov. 2017.

[36] T. S. Kumar and V. Nagarajan, "Combining LBP and contourlet features for image retrieval," in *Proc. Int. Conf. Commun. Signal Process.*, Apr. 2016, pp. 1193–1196.

[37] J. Zhou, X. Liu, W. Liu, and J. Gan, "Image retrieval based on effective feature extraction and diffusion process," *Multimedia Tools Appl.*, vol. 78, no. 5, pp. 6163–6190, Mar. 2019.

[38] A. Nazir and K. Nazir, "An efficient image retrieval based on fusion of low-level visual features," 2018, *arXiv:1811.12695*. [Online]. Available: http://arxiv.org/abs/1811.12695

[39] V. Naghashi, "Co-occurrence of adjacent sparse local ternary patterns: A feature descriptor for texture and face image retrieval," *Optik*, vol. 157, pp. 877–889, Mar. 2018.

[40] N. Kingsbury, "Complex wavelets for shift invariant analysis and filtering of signals," *Appl. Comput. Harmon. Anal.*, vol. 10, no. 3, pp. 234–253, May 2001.

[41] A. Vo and S. Oraintara, "A study of relative phase in complex wavelet domain: Property, statistics and applications in texture image retrieval and segmentation," *Signal Process., Image Commun.*, vol. 25, no. 1, pp. 28–46, Jan. 2010.

[42] Z. Guo, L. Zhang, and D. Zhang, "Rotation invariant texture classification using LBP variance (LBPV) with global matching," *Pattern Recognit.*, vol. 43, no. 3, pp. 706–719, Mar. 2010.

[43] Z. Guo, L. Zhang, and D. Zhang, "A completed modeling of local binary pattern operator for texture classification," *IEEE Trans. Image Process.*, vol. 19, no. 6, pp. 1657–1663, Jun. 2010.

[44] D.-S. Huang, W. Jia, and D. Zhang, "Palmprint verification based on principal lines," *Pattern Recognit.*, vol. 41, no. 4, pp. 1316–1328, Apr. 2008.

[45] P. Brodatz, *Textures: A Photographic Album for Artists and Designers*. New York, NY, USA: Dover, 1966.

[46] *Corel 1000 and Corel 10000 Image Database*. Accessed: Dec. 2020. [Online]. Available: http://sipi.usc.edu/database/

[47] University of Southern California, Los Angeles, CA, USA. *Signal and Image Processing Institute*. Accessed: Dec. 2020. [Online]. Available: http://sipi.usc.edu/database/

[48] MIT Vision and Modeling Group, Cambridge. U.K. *Vision Texture*. Accessed: Dec. 2020. [Online]. Available: http://vismod.media.mit.edu/pub/

[49] M. Subrahmanyam, R. P. Maheshwari, and R. Balasubramanian, "Local maximum edge binary patterns: A new descriptor for image retrieval and object tracking," *Signal Process.*, vol. 92, no. 6, pp. 1467–1479, Jun. 2012.

[50] D. Jiang and J. Kim, "Texture image retrieval using DTCWT-SVD and local binary pattern features," *JIPS*, vol. 13, no. 6, pp. 1628–1639, 2017.

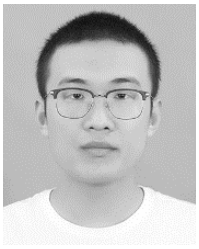

HENGBIN WANG was born in Linyi, China, in 1996. He received the B.S. degree in communication engineering from Shandong Jianzhu University, in 2018, where he is currently pursuing the master's degree in control science and engineering. His current research interest includes image processing, especially on texture image retrieval.

HUAIJING QU received the B.S. degree in electric engineering from the Shandong University of Technology, Jinan, China, in 1986, and the Ph.D. degree in signal and information processing from Shandong University, Jinan, in 2009. He is currently a full-time Associate Professor with the School of Information and Electric Engineering, Shandong Jianzhu University, Jinan. His research interests include multi-scale and multidirectional image processing, image retrieval, image fusion, and pattern recognition.

JIA XU was born in Heze, China, in 1996. He received the B.S. degree in communication engineering from Shandong Jianzhu University, in 2018, where he is currently pursuing the master's degree in control engineering. His current research interest includes image processing, especially on texture image retrieval.

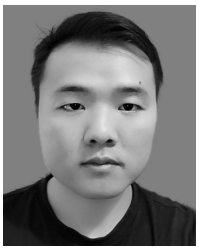

JIWEI WANG received the B.S. degree in automation from the Anyang Institute of Technology, in 2018. He is currently pursuing the M.S. degree in control science and engineering with Shandong Jianzhu University. His current research interests include computer vision and image fusion.

YANAN WEI was born in Jining, China, in 1995. She received the B.S. degree in computer science and technology from the Qilu University of Technology, in 2019. She is currently pursuing the master's degree in control engineering with Shandong Jianzhu University. Her current research interest includes image processing, especially image fusion.

ZHISHENG ZHANG was born in Henan, China, in 1995. He received the B.S. degree from the Henan Institute of Engineering, in 2019. He is currently pursuing the master's degree in control science and engineering with Shandong Jianzhu University. His current research interest includes image retrieval.